Refereed Proceedings

The 13th International Conference on Fluidization - New Paradigm in Fluidization Engineering

Engineering Conferences International *Year* 2010

NUMERICAL STUDY OF BUBBLE HYDRODYNAMICS FOR GAS-SOLID FLUIDIZED BEDS WITH AND WITHOUT HORIZONTAL TUBES

Teklay W. Asegehegn* Hans Joachim Krautz†

*Brandenburg University of Technology Cottbus, teklay.asegehegn@tu-cottbus.de

†Brandenburg University of Technology Cottbus

NUMERICAL STUDY OF BUBBLE HYDRODYNAMICS FOR GAS-SOLID FLUIDIZED BEDS WITH AND WITHOUT HORIZONTAL TUBES

Teklay Weldeabzgi Asegehegn*, Hans Joachim Krautz
Chair of Power Plant Technology, Brandenburg University of Technology Cottbus
Walther-Pauer-Strasse 5, 03046 Cottbus, Germany
* Tel.: +49 (0) 355-695060, Mail: teklay.asegehegn@tu-cottbus.de

ABSTRACT

The paper deals with numerical simulations using the Eulerian-Eulerian Two Fluid Model (TFM) of 2D gas-solid bubbling fluidized beds with and without immersed horizontal tubes. The bubble diameters and rise velocities obtained from the simulations presented good agreement when compared with experiments and correlations available in the literature. The presence of horizontal tubes inside the bed was found to be the main cause of bubble breakup, which eventually reduce the bubble diameter and rise velocity.

INTRODUCTION

Fluidized beds are widely applied in process and chemical industries such as combustion, drying, polymerization, cracking of hydrocarbons, heat exchange, etc. In many applications tubes are usually inserted to enhance the rate of heat transfer and chemical conversion. Despite the significant influence of such immersed tubes is on the bubble hydrodynamics, many literatures have been concerned mainly on the improvement of the heat transfer coefficient between the tubes and the emulsion phase. This is possibly due to the complexity and cost of experimental procedures for measuring bubble properties within complex bed geometries. In recent years, due to rapid growth of computer capacity, numerical simulation is becoming a powerful tool in determining the macro- and microscopic phenomena of gas-solid fluidized beds. Numerical studies are more flexible and less expensive especially when one has to perform parametric investigations for different bed geometries and operating conditions. In general, two types of computer models are widely applied today, the Two Fluid Model (TFM) based on the Eulerian-Eulerian approach (1) and the Discrete Particle Model (DPM) based on the Eulerian-Lagrangian approach (2; 3). DPM is a more fundamental approach for fluidized bed applications; however, the need of very high computational efforts has made it more prohibitive and limited to only few particles and very small fluidized beds. On the other hand the TFM, which requires less computational time, is the realistic approach for parametric investigation of fluidized beds of engineering scales (4; 5).

Since the first breakthrough of the TFM reported by Anderson and Jackson (1), many studies are published in the open literature regarding its implementation for

gas-solid fluidized beds. The latest development of the model came from the Kinetic Theory of Granular Flow (KTGF). This approach, which is the extension of kinetic theory of dense gases (6), was applied first to granular flows by Jenkins and Savage (7) and Lun et al. (8). Later Ding and Gidaspow (9) and Gidaspow (10) applied it to dense gas-solid fluidized beds. Despite these developments, the application and validity of the model for beds with internals are not sufficiently reported. Bouillard et al. (11) investigated the porosity distribution around an immersed rectangular tube. Gamwo et al. (12) studied the general solid flow patterns for a bed with staggered horizontal tubes. Gustavsson and Almstedt (13) investigated bubble properties at different pressure levels using general curvilinear coordinate systems. Yurong et al. (14) applied a body fitted coordinate system in order to match the boundaries of the immersed tubes. Pain et al. (15) used finite element method formulation and perform simulation with a single cylindrical obstruction. In this study the TFM model was used to investigate the influence of immersed horizontal tubes on bubble hydrodynamics. The mean bubble diameter and rise velocity across the bed height were calculated and compared with experimental results and correlations available in the literature.

NUMERICAL MODELLING

The TFM implemented in Fluent 6.3, with closure equations based on the KTGF were used (16). Table 1 shows the governing equations and closure models used in this work. Three different tube arrangements were investigated, staggered (S3), in-line (I3) and without immersed tubes (NT). The beds were 2D, 0.2 m wide and 1 m high. The detail dimensions can be found in Hull et al. (17) and the staggered arrangement is reproduced in figure 1. A triangular mesh for the beds with tubes and quad mesh for the bed without tubes of 8 mm size was used with slight refinement of up to 5 mm near the tube surfaces to capture the higher velocity gradients there. The QUICK and second order upwind were used for the spatial discretization of the continuity and momentum equations respectively while time was discretized using first order implicit. The Phase-Coupled SIMPLE algorithm was used for the pressure-velocity coupling. Table 2 shows additional simulation parameters used in this work.

Table 1: Governing and closure equations (KTGF)

Mass conservation (q=g for gas, and q=s for solid)

$$\frac{\partial(\varepsilon_q\rho_q)}{\partial t}+\nabla\cdot(\varepsilon_q\rho_q\mathbf{u}_q)=0$$

Momentum conservation

$$\frac{\partial(\varepsilon_g\rho_g\mathbf{u}_g)}{\partial t}+\nabla\cdot(\varepsilon_g\rho_g\mathbf{u}_g\mathbf{u}_g)=\nabla\cdot(\boldsymbol{\tau}_g)-\varepsilon_g\nabla P-\beta(\mathbf{u}_g-\mathbf{u}_s)+\varepsilon_g\rho_g\mathbf{g}$$

$$\frac{\partial(\varepsilon_s\rho_s\mathbf{u}_s)}{\partial t}+\nabla\cdot(\varepsilon_s\rho_s\mathbf{u}_s\mathbf{u}_s)=\nabla\cdot(\boldsymbol{\tau}_s)-\varepsilon_s\nabla P-\nabla P_s+\beta(\mathbf{u}_g-\mathbf{u}_s)+\varepsilon_s\rho_s\mathbf{g}$$

Conservation of solid fluctuating kinetic energy*

$$\frac{3}{2}\left(\frac{\partial(\varepsilon_s\rho_s\Theta)}{\partial t}+\nabla\cdot(\varepsilon_s\rho_s\mathbf{u}_s\Theta)\right)=(-P_s\mathbf{I}+\boldsymbol{\tau}_s):\nabla\mathbf{u}_s-\nabla\cdot\mathbf{q}-\gamma-J$$

*In this work the algebraic form of this equation was used (18).

Closure equations

Parameter	Model (Fluent)	Ref.
Solid viscosity	Gidaspow	(10)
Solid bulk viscosity	Lun et al.	(8)
Frictional viscosity	Schaeffer	(19)
Frictional pressure	Johnson et al.	(20)
Solid pressure	Lun et al.	(8)
Radial distr. function	Lun et al.	(8)
Drag law	Gidaspow	(10)

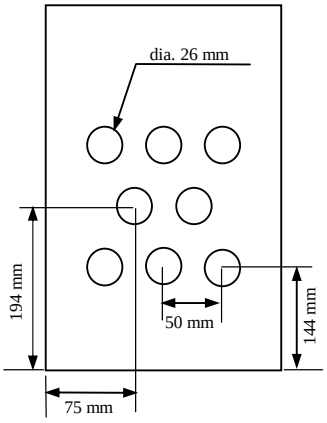

Figure 1. Geometry for the staggered arrangement. Drawing is not to scale.

Table 2: Physical properties and simulation parameters

	Values	Source
Gas density	1.2 kg/m^3	Fluent
Gas viscosity	1.7894 x 10^{-5} Pa·s	Fluent
Particle density	2700 kg/m^3	Estimated
Particle diameter	0.230 mm	(17)
Minimum fluidization velocity	0.047 m/s	(17)
Minimum fluidization void fraction	0.42	Estimated
Bed height at minimum fluidization	0.3 m	(17)
Restitution coefficient	0.9	(21)
Superficial velocity	0.15 m/s	(17)
Maximum particle packing limit	0.63	Fluent
Specularity coefficient	0.25	(20)
Time step size	5x10^{-5} s	

Boundary and Initial Conditions

At the inlet the velocity inlet boundary condition with uniform superficial velocity of the gas phase was set. At the outlet the pressure outlet boundary condition was set for the mixture phase. In addition, the height of the free board was made long enough such that a fully developed flow was achieved for the gas phase. At the walls the gas phase was assumed to have a no slip boundary condition while the solid phase was assumed to have a partial slip boundary condition (22). The initial conditions of the bed were set to the minimum fluidization condition with all parameters at minimum fluidization as given in table 2.

RESULTS AND DISCUSSION

The simulations were performed for 10 s of real flow time. The first 3 s were neglected to reduce the start-up effect. Thus, all the results reported in this work were averaged over the last 7 s of real flow time. The bubble properties were calculated from the volume fraction contour produced by Fluent. There is no clear definition of bubble boundaries, however, many previous investigators defined the boundary to be 0.8 for the gas volume fraction (23) and this definition was adopted in this study as well. The beds were divided into equal horizontal sections of 0.01 m height. Taking into account the bubble breakup and coalescence, the bubble properties like projected area, centroid and vertical and horizontal extremes were calculated for each bubble in each section in time interval of 0.02 s.

It was observed that tubes were the main cause for bubble splitting. Small bubbles were usually formed at the bottom of the bed. They rise and grew by coalescence until they reached the first row of the tubes which then split and further grew by coalescence until they reach the next row of tubes. This continued until the last row of tubes after which large bubbles were formed up to they finally erupted at the top of the bed. The detail simulation results of bubble aspect ratio, bubble diameter, and bubble rise velocity are discussed below.

Bubble Aspect Ratio

Aspect ratio is an important characteristic of a bubble since it strongly influences the bubble's hydrodynamics. It provides an approximate bubble shape (circularity in 2D or sphericity in 3D). To examine the influence of tubes on the bubble shape the time averaged bubble aspect ratios were calculated for the three beds. The aspect ratio is defined as the ratio of the vertical (d_y) and horizontal (d_x) extremes, figure 2.

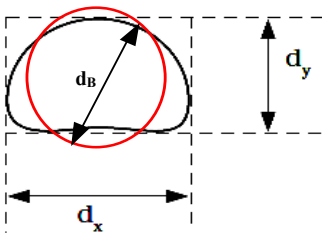

Figure 2. Bubble dimensions

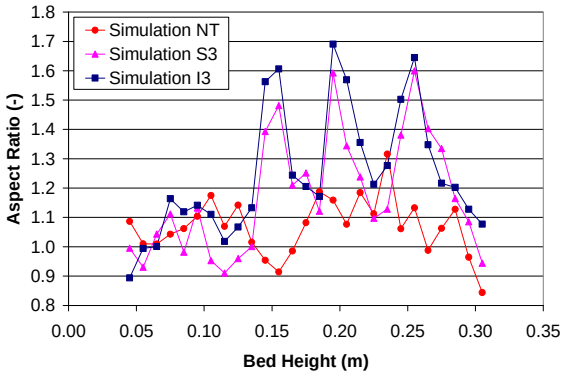

Figure 3. Bubble aspect ratio with bed height

Figure 3 shows the time averaged bubble aspect ratio for the three bed geometries considered. It was found that for the bed without tubes the aspect ratio is nearly unity throughout the bed height. This showed that the bubble shape remains almost circular. However, for beds with immersed tubes bubbles were observed to be longer vertically when they pass between tube rows and nearly circular when they are far from the tube rows. The elongation of bubbles in the vertical direction could be associated to two possible mechanisms of bubble motion observed. The first mechanism occurred when the horizontal extreme (d_x) of a bubble is greater than the horizontal separation between two tubes in a row. In this case the bubble squeezed or deformed as it passed between the tubes due to the decrease in the area of passage. This resulted in increased vertical extreme (d_y) as the area of the bubble has to be conserved, provided that no splitting or coalescence is taking place during the process. The second mechanism was the stretching of a bubble as it moved over the surface of the tubes. This phenomenon was observed regardless the size of a bubble. When a bubble moved over the surface of a tube, it stretched vertically due to the velocity difference observed between the bubble surface in contact with the tube and the rest. The surface of the bubble which was in contact with the tubes had lower velocity as compared to the rest part of the bubble. Hence the relative velocity resulted from this velocity difference stretched the bubble in its direction. The reason for the lower velocity of the bubble surface in contact with the tubes could be due to the no slip boundary condition imposed on the walls of the bed. However, experimental verification is needed if such phenomenon can actually happen or are results of the numerical approximations.

Bubble Diameter

The bubble diameter was calculated from the area equivalent using equation 1.

$$d_B = \sqrt{\frac{4A_B}{\pi}} \qquad (1)$$

Figure 4 shows the time averaged bubble diameters from the simulations and their comparison with experimental data and available correlations. In figure 4a the results for the bed without immersed tubes were compared with equations given by Hull et al. (17) and Shen et al. (24). The numerical simulation was in good agreement with the expressions. The two expressions are basically equivalent except for their estimation of the initial bubble size. This was mainly the source of the slight overprediction by the correlation of Shen et al. (24).

In figure 4b the results for the staggered tube arrangement and comparison with experimental data of Hull et al. (17) are presented. The simulation is in good agreement with the experiments in the majority of the bed. The difference between the two results occurred near the lower and upper parts of the tube rows. The slight underprediction of the simulation on the lower side of the tube rows can be explained due to the fact that, small bubbles were observed to form at the bottom of the tubes which resulted in significant change of the bubble hydrodynamics around the tube bank region. This was explained in our previous study (25). On the other hand the slight overprediction of the simulation results on the upper side of the tube rows is not clearly known and it needs further simulations and validation with experiments. In figure 4c the comparison between the mean bubble diameters for the three beds is shown. No major difference between the inline and staggered tube arrangements were observed. For both beds with tubes the mean bubble diameter is smaller than the same bed without tubes. This is due to the higher rate of bubble splitting resulted form the presence of tubes which eventually reduced the bubble size.

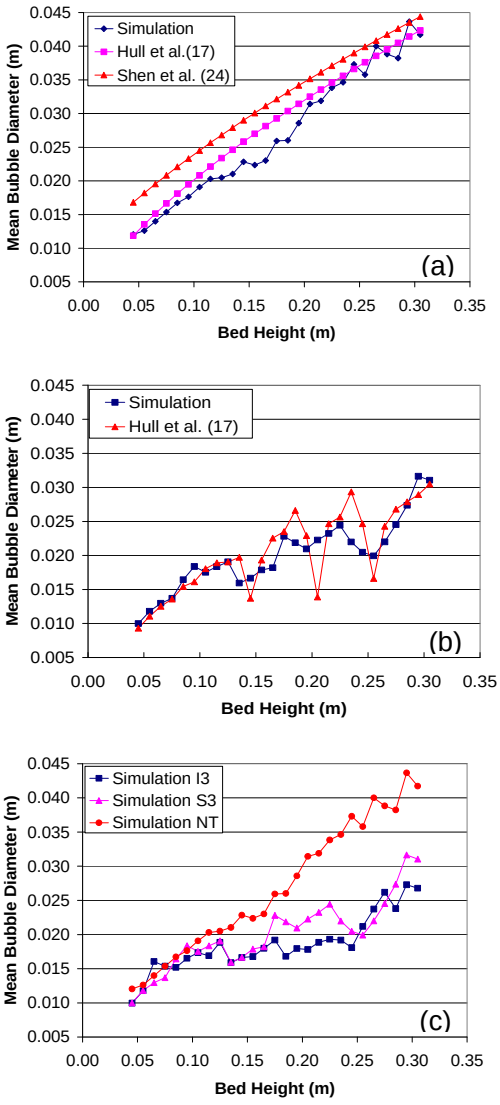

Figure 4. Mean bubble diameter versus bed height above distributor (a) NT, (b) S3, (c) all

Bubble Rise Velocity

The bubble rise velocity was calculated from the difference in the vertical coordinate of the centriod between consecutive time frames and dividing by the time interval. Figure 5 shows the time average bubble rise velocities. In figure 5a the simulation results of the bed without internals were compared with correlations of Shen et al. (24). The simulation predicted larger bubble on the upper part of the bed. In figure 5b comparison of the simulation results with experimental data of Hull et al. (17) for the staggered tube arrangement is shown. The results showed good agreement. Similar to the mean diameters, the rise velocities were lower at the bottom of the tubes and were explained in our previous publication (25). The higher velocity predicted by the simulation on the upper part of the tube rows can be explained partly due to the two bubble motion mechanisms explained above. As a result of the elongation of a bubble and stretching over the surface of the tubes, the centroid of the bubble moved farther than expected if it was circular. Such phenomena were not reported on the experimental study of Hull et al. (17). In their explanation they associated the lower rise velocity at the upper part of the tube rows to the decrease in bubble diameter due to splitting. In fact this was also observed in the simulation results, figure 5b, and c. However, the simulation showed higher rise velocity as a bubble moved between the tubes. This was seen to be the result of changing the bubble shape in these regions. In general in the tube bank regions of the fluidized beds with immersed tubes the bubble rise velocity depends not only on the bubble size but also on the bubble shape. The comparison of the mean rise velocities in figure 5c shows that, the mean bubble rise velocity of the bed without internals is higher than the beds with internals. This is mainly due to the decrease in bubble size of beds with internals. Regarding the two tube arrangements, the inline predicted slightly higher bubble rise velocity on upper part of the bed. This could be due to the unrestricted motion of bubbles between the tube columns. This was also shown as higher aspect ratio of the bubbles, figure 3.

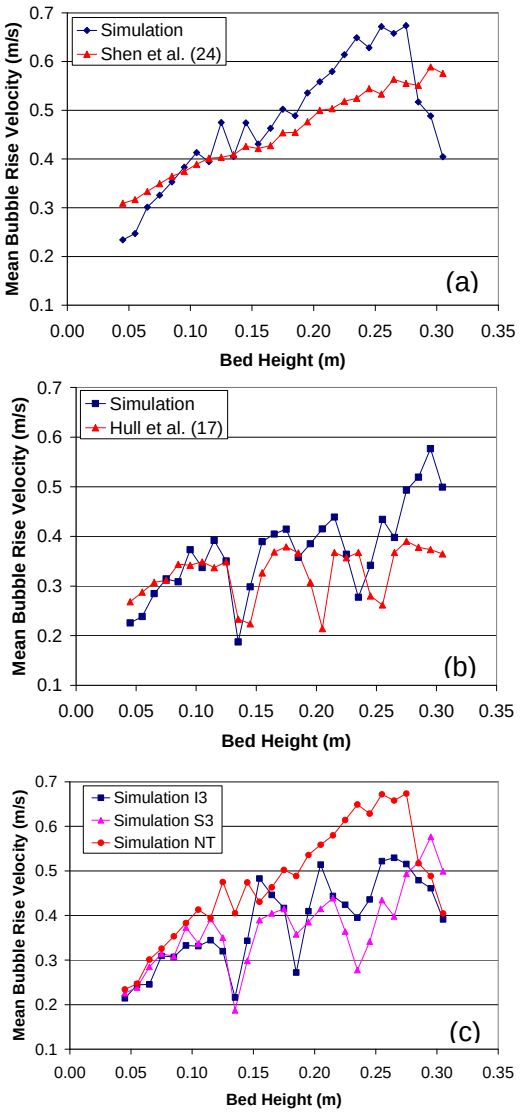

Figure 5. Mean bubble rise velocity versus bed height above distributor, (a) NT, (b) S3, (c) all

CONCLUSIONS

Hydrodynamic simulations of dense gas-solid bubbling fluidized beds with and without immersed tubes were performed. The Eulerian-Eulerian Two Fluid Model was acceptably predicted the mean bubble characteristics. For beds with immersed tubes, the presence of horizontal tubes was the main cause of bubble breakup which eventually reduces the mean bubble diameter and rise velocity. The bubble aspect ratio predicted by the simulations indicated that bubbles were no more circular in the tube bank region as compared to beds without internals which remain nearly circular. This variation of bubble shape was seen to alter significantly the bubble rise velocities in the vicinity of the tube banks. The complex mechanism of bubble movement around the tubes, which alters the bubble aspect ratio, was observed to be the main source of mismatching between the simulation and experiments. The mismatching could be also a result of data extraction and numerical approximations as the two studies were performed by two different investigators at two different times. In any case, the numerical simulations showed an intensive investigation is needed to verify the mechanism of bubble motion in the presence of obstacles. In relation to this the mechanism of local fluidization or bubble formation at the lower part of the tubes should be well studied. In addition, further experimental and numerical studies with more dense tube arrangements are necessary for better understanding of the influence of immersed tubes. In general the Two Fluid Model is capable of predicting the main characteristics of bubble behavior with complex geometries. It is a promising tool for parametric investigation of fluidized bed reactors. However, intensive experimental validations are required before using it as a commanding method for scaling up and design procedures of these systems.

ACKNOWLEDGEMENT

The authors would like to gratefully acknowledge to Brandenburg Ministry of Higher Education, Research and Culture and Brandenburg University of Technology Cottbus for their financial support of this work.

NOTATION

Symbols:

A_B	Area of a bubble, m^2
d_B	Bubble diameter, m
g	Gravitational acceleration, m/s^2
$\boldsymbol{I}$	Unit tensor
J	Transfer of random fluctuations kinetic energy, Pa/s
P	Pressure, Pa
$\boldsymbol{q}$	Diffusive flux of granular energy, Pa/s
t	Time, s
u	Velocity, m/s

Greek letters:

β	Inter-phase drag coefficient, $kg/m^3/s$
ε	Volume fraction
γ	Dissipation of fluctuating energy, Pa/s
Θ	Granular temperature, m^2/s^2
ρ	Density, kg/m^3
τ	Shear stress tensor, N/m^2

Subscripts:

g	Gas phase
s	Solid phase

REFERENCES

1. Anderson, T. B., and Jackson, R.: I & EC Fundamentals **6** (1967), 527-539
2. Tsuji, Y., Kawaguchi, T., and Tanaka, T.: Powder Technol. **77** (1993), 79-87
3. Hoomans, B. P. B., Kuipers, J. A. M., Briels, W. J., and Van Swaaij, W. P. M.: Chem. Eng. Sci. **51** (1996), 99-118
4. Van Wachem, B.G.M., Schouten, J. C., van den Bleek, C. M., Krishna, R., and Sinclair, J. L.: AIChE Journal **47** (2001), 1035-1051
5. Van der Hoef, M. A., van Sint Annaland, M., Deen, N. G., and Kuipers, J. A. M.: Annu. Rev. Fluid Mech. **40** (2008), 47-70
6. Chapman, S., and Cowling, T. G.; (1970), The Mathematical Theory of Non-Uniform Gases, Cambridge University press, Cambridge.
7. Jenkins, J. T., and Savage, S.B.: J. of Fluid Mech. **130** (1984), 187-202
8. Lun, C.K.K., Savage, S.B., Jeffrey, D.J., and Chepurniy, N.: J.Fluid Mech. **140** (1984), 223-256
9. Ding, J. and Gidaspow, D.: A.I.Ch.E Journal **36** (1990), 523-538
10. Gidaspow, D.: (1994), Multiphase Flow and Fluidization: Continuum and Kinetic Theory Descriptions, Academic Press, Boston
11. Bouillard, J. X., Lyczkowski, and Gidaspow, D.: AIChE Journal **35** (1989), 908-922
12. Gamwo, I. K., Soong, Y., and Lyczkowski, R. W.: Powder Technol. **103** (1999), 117-129
13. Gustavsson, M., and Almstedt, A. E.: Chem. Eng. Sci. **55** (2000), pp. 857-866
14. Yurong, H., Huilin, L., Qiaoqun, S., Lidan, Y., Yunhua, Z., Gidaspow, D., and Bouillard, J.: Powder Technol. **145** (2004), 88-105
15. Pain, C.C., Mansoorzadeh, S., and de Oliveira, C. R. E.: Int. J. Multiphase Flow **27** (2001), 527-551
16. Fluent Inc.: FLUENT 6.3 User's Guide, (2006), 23.5 Eulerian Model Theory
17. Hull, A. S., Chen, Z., Fritz, J. W., and Agarwal, P. K.: Powder Technol. **103** (1999), 230-242
18. Syamlal, M., Rogers, W., and O'Brien, T. J.: (1993), MFIX Documentation: Theory Guide, National Technical Information Service, Springfield, VA, DOE/METC-94/1004 (DE94000087)
19. Schaeffer, D.G.: J. Diff. Eq., **66** (1987), 19-50
20. Johnson, P. C., Nott, P., and Jackson, R.: J. Fluid Mech. **210** (1990), 501-535
21. Taghipour, F., Ellis, N., and Wong, C.: Chem. Eng. Sci., **60** (2005), 6857-6867
22. Johnson, P. C., and Jackson, R.: J. Fluid Mech. **176** (1987), 67-93
23. Hulme, I., Clavelle, E., van der Lee, L., and Kantzas, A.: Ind. Eng. Chem. Res. **44** (2005), 4254-4266
24. Shen, L., Johnsson, F., and Leckner, B.: Chem. Eng. Sci. **59** (2004), 2607-2617
25. Asegehegn, T. W., and Krautz, H. J.: Hydrodynamic Simulation of Gas-Solid Bubbling Fluidized Bed Containing Horizontal Tubes, Proceedings of the 20th International Conference on Fluidized Bed Combustion, May 18-20, (2009), 864-869, Xian, China.